

4-1-1996

Oscillatory Doubly Diffusive Convection in a Finite Container

Adam S. Landsberg

Claremont McKenna College; Pitzer College; Scripps College

Edgar Knobloch

University of California - Berkeley

Recommended Citation

Landsberg, A.S., and E. Knobloch. "Oscillatory Doubly Diffusive Convection in a Finite Container." *Physical Review E* 53.4 (1996): 3601–3609. DOI: 10.1103/PhysRevE.53.3601

This Article is brought to you for free and open access by the W.M. Keck Science Department at Scholarship @ Claremont. It has been accepted for inclusion in WM Keck Science Faculty Papers by an authorized administrator of Scholarship @ Claremont. For more information, please contact scholarship@cuc.claremont.edu.

Oscillatory doubly diffusive convection in a finite container

A.S. Landsberg* and E. Knobloch

Department of Physics, University of California, Berkeley, California 94720

(Received 13 March 1995)

Oscillatory doubly diffusive convection in a large aspect ratio Hele-Shaw cell is considered. The partial differential equations are reduced via center-unstable manifold reduction to the normal form equations describing the interaction of even and odd parity standing waves near onset. These equations take the form of the equations for a Hopf bifurcation with approximate D_4 symmetry, verifying the conclusions of the preceding paper [A.S. Landsberg and E. Knobloch, Phys. Rev. E **53**, 3579 (1996)]. In particular, the amplitude equations differ in the limit of large aspect ratios from the usual Ginzburg-Landau description in having additional nonlinear terms with $O(1)$ coefficients. Numerical simulations of the amplitude equations for experimental parameter values are presented and compared with the results of recent experiments by Predtechensky *et al.* [Phys. Rev. Lett. **72**, 218 (1994); Phys. Fluids **6**, 3923 (1994)].

PACS number(s): 47.20.Bp, 47.20.Ky, 03.40.Kf

I. INTRODUCTION

In the companion paper [1] we argue that the amplitude equations describing the bifurcation to traveling waves in a finite but large aspect ratio container are more complex than suggested by the usual Ginzburg-Landau description. In particular we argue that the correct description of the initial instability must be based on the even and odd parity standing waves, which are the only modes that bifurcate from the trivial state in such a container. In large aspect ratio systems the even and odd modes are nearly degenerate, indicating that their interaction cannot be neglected. By considering the interaction of the first two modes to go unstable we derived amplitude equations of the form

$$\frac{dz_m}{dt} = \delta_m z_m + K_1 |z_m|^2 z_m + K_2 |z_{m+1}|^2 z_m + K_3 \bar{z}_m z_{m+1}^2, \quad (1a)$$

$$\frac{dz_{m+1}}{dt} = \delta_{m+1} z_{m+1} + K'_1 |z_{m+1}|^2 z_{m+1} + K'_2 |z_m|^2 z_{m+1} + K'_3 \bar{z}_{m+1} z_m^2. \quad (1b)$$

Here (z_m, z_{m+1}) are the (complex) amplitudes of the first two modes, $\delta_m \equiv \mu_m + i\omega_m$, $\delta_{m+1} \equiv \mu_{m+1} + i\omega_{m+1}$ represent their linear growth rates and frequencies, and K'_1, K'_2, K'_3 are complex coefficients that are close to K_1, K_2, K_3 because of the near degeneracy of the two modes. The relevance of Eqs. (1a) and (1b) to the study of oscillatory instabilities in finite containers was recognized already by Bestehorn, Friedrich, and Haken [2] and Nagata [3]. The amplitude equations are to be thought of as describing the double Hopf bifurcation with 1:1 resonance and ap-

proximate D_4 symmetry owing to the near degeneracy between the two modes. The equations have stationary solutions of the form $(z_m, 0)$, $(0, z_{m+1})$ corresponding to the two types of standing waves. Generically, such waves take the form of "chevrons," i.e., of patterns consisting of left-traveling waves in the left half of the container and right-traveling waves in the right half (or vice versa), satisfying the requirement that they are either even or odd under reflections about the middle. As the bifurcation parameter is increased these solutions typically lose stability at secondary bifurcations to nonsymmetric stationary states (z_m, z_{m+1}) , $z_m z_{m+1} \neq 0$, corresponding to various types of propagating patterns, as described in [1]. In order to compare this formulation of the problem with the Ginzburg-Landau description it is illuminating to write Eqs. (1a) and (1b) in terms of the amplitudes (v, w) of left- and right-traveling waves. The appropriate transformation is linear, $z_m = v + \bar{w}$, $z_{m+1} = v - \bar{w}$, and yields, in the large aspect ratio limit,

$$\frac{dv}{dt} = (\lambda + i\omega)v + \Delta \bar{w} + a|v|^2 v + b(|v|^2 + |w|^2)v + c\bar{v}w^2, \quad (2a)$$

$$\frac{dw}{dt} = (\lambda - i\omega)w + \bar{\Delta} \bar{v} + \bar{a}|v|^2 w + \bar{b}(|v|^2 + |w|^2)w + \bar{c}\bar{v}^2 \bar{w}, \quad (2b)$$

where $\lambda + i\omega = \frac{1}{2}(\delta_m + \delta_{m+1})$, $\Delta = \frac{1}{2}(\delta_m - \delta_{m+1})$, $a = K_1 - K_2 - 3K_3$, $b = K_1 + K_2 + K_3$, and $c = K_1 - K_2 + K_3$. In writing these equations we have ignored any differences between K_j and K'_j , $j = 1, 2, 3$. Note that we have chosen z_m to be even under reflection, $(v, w) \rightarrow (\bar{w}, \bar{v})$, while z_{m+1} is odd.

Equations (2a) and (2b) differ from the usual Ginzburg-Landau equations in the presence of new nonlinear terms $(\bar{v}w^2, \bar{v}^2\bar{w})$ as well as the linear terms $(\Delta\bar{w}, \bar{\Delta}\bar{v})$. The presence of the latter is a natural consequence of the breaking of translation invariance [4]; these

*Permanent address: School of Physics, Georgia Institute of Technology, Atlanta, GA 30332.

terms have a small coefficient and thus represent a small perturbation of the Ginzburg-Landau equations for an unbounded system [5]. In [1] we argue, however, that the coefficients of the new cubic terms should be of order unity, and hence that their appearance does *not* represent a perturbation of the equations for the unbounded system.

In the present paper we focus on the problem of doubly diffusive convection in a large aspect ratio Hele-Shaw cell. The motivation for this study is twofold. First, we seek to demonstrate, by explicit computation on a continuum system in a box of aspect ratio L , that the dynamics near onset is described by Eqs. (1a) and (1b), and that, in the limit $L \rightarrow \infty$, all the coefficients of the nonlinear terms do remain finite. In particular we show that the coefficient c in Eqs. (2a) and (2b) also remains finite. The Hele-Shaw problem is particularly well suited for this purpose, owing to the analytical tractability of the corresponding linear stability problem, and in particular the simple form of the unstable modes. Second, recent and extensive experimental studies of this type of system by Predtechensky *et al.* [6] have provided a wealth of data on the behavior of this system in the weakly nonlinear regime. Given that the dynamics described by Eqs. (1a) and (1b) show good *qualitative* resemblance with the behavior found in binary fluid convection [7, 8] and in numerical simulations [9, 10], including the so-called confined and blinking states as well as repeated transients, a calculation of the actual coefficient values offers the scope for a comparison between theory and experiment. Moreover, by means of these analytic calculations we can address the question of whether or not the “standard” model for this doubly diffusive system, in which “secondary” effects like cross diffusion are neglected, suffices to capture the experimentally observed behavior.

The paper is organized as follows. In Sec. II we describe the problem, introduce the governing partial differential equations, and use these to derive Eqs. (1a) and (1b), obtaining explicit expressions for the coefficients in terms of the physical parameters. In Sec. III we present numerical results obtained by integrating Eqs. (1a) and (1b) for parameter values corresponding to those of the experiment. Our conclusions are summarized in Sec. IV.

II. DOUBLY DIFFUSIVE CONVECTION IN HELE-SHAW GEOMETRY

The recent experiments by Predtechensky *et al.* [6] on doubly diffusive convection employ a thin *isothermal* rectangular cell. Instead of using thermal forcing to destabilize the system, a second diffusing component with a slightly higher diffusivity and lower molecular weight is fed in from the top. This component competes with a stabilizing gradient of a lower diffusivity component fed in from the bottom. Both the top and bottom are in contact with fixed concentration reservoirs of the respective components via gel-filled membranes that allow diffusion but no flow. In this way fixed concentration boundary conditions are achieved. In the following we use the subscripts t, s to refer to the destabilizing and stabilizing components, respectively.

A. Model equations and general considerations

The governing equations for the above experiment can be written in the nondimensional form:

$$\frac{1}{\sigma} [\partial_t \nabla^2 \psi + J(\psi, \nabla^2 \psi)] = R_t \theta_x - R_s \phi_x - \nabla^2 \psi, \quad (3a)$$

$$\partial_t \theta + J(\psi, \theta) = \partial_x \psi + \nabla^2 \theta, \quad (3b)$$

$$\partial_t \phi + J(\psi, \phi) = \partial_x \psi + \tau \nabla^2 \phi, \quad (3c)$$

where ψ is the stream function, and θ, ϕ denote the departures of the two concentration fields from their respective conduction profiles. The operator J satisfies $J(u, v) = \partial_x u \partial_z v - \partial_z u \partial_x v$. The Rayleigh numbers R_t, R_s provide a nondimensional measure of the imposed destabilizing and stabilizing concentration gradients, and are positive. The parameter τ denotes the diffusivity ratio D_s/D_t ($0 < \tau < 1$), while σ denotes the ratio ν/D_t . Here ν is the coefficient of the Darcy viscosity term ($-\nabla^2 \psi$) used here instead of the usual viscosity (which would appear as $\nabla^4 \psi$ in the first equation), as is appropriate for the Hele-Shaw (thin cell) geometry. The endwalls lie at $x = 0, L$, and the bottom and top walls at $z = 0, 1$. We refer to L as the aspect ratio, and assume that it is large. The boundary conditions appropriate to the experiment are

$$\theta = \phi = 0 \quad \text{at } z = 0, 1, \quad (4a)$$

$$\partial_x \theta = \partial_x \phi = 0 \quad \text{at } x = 0, L, \quad (4b)$$

$$\psi = 0 \quad \text{at } x = 0, L; z = 0, 1. \quad (4c)$$

These conditions correspond, respectively, to fixed concentrations at top and bottom, no concentration flux through the endwalls, and no fluid flux through the top, bottom, or sides. Note that since the use of a Darcy viscosity term changes the order of the equation, there are fewer boundary conditions imposed on ψ than usually.

The problem as posed has two discrete symmetries, labeled κ_1, κ_2 . The first results from the manifest left-right reflection invariance of the system:

$$\kappa_1 : x \rightarrow L - x, \quad \psi \rightarrow -\psi. \quad (5)$$

The second, a midplane reflection symmetry,

$$\kappa_2 : z \rightarrow 1 - z, \quad \psi \rightarrow -\psi, \quad \theta \rightarrow -\theta, \quad \phi \rightarrow -\phi, \quad (6)$$

arises as a consequence of the Boussinesq approximation used to derive (3a)–(3c), and is thus peculiar to this particular model. However, the presence of this additional (midplane) symmetry does not alter the form of the normal form equations. It should be noted that the boundary conditions (4a)–(4c) are of Neumann type and hence introduce additional “hidden” symmetries into the problem. It can be shown, however, that these symmetries do not introduce any additional restrictions on the normal form for the Hopf bifurcation [11].

B. Linear theory

The first step of the derivation involves solving the linearized version of Eqs. (3a)–(3c). With the boundary conditions (4a)–(4c), the oscillatory instability occurs at $R_t = R_t^{\text{Hopf}}$ with the frequency Ω_{Hopf} . These are given by (cf. [6,12,13])

$$R_t^{\text{Hopf}} = \frac{\sigma + k^2\tau}{\sigma + k^2} R_s + \frac{k^4(1 + \tau)(\sigma + k^2\tau)}{\sigma k_x^2}, \quad (7a)$$

$$\Omega_{\text{Hopf}}^2 = \frac{\sigma(1 - \tau)k_x^2}{\sigma + k^2} R_s - \tau^2 k^4, \quad (7b)$$

where $k_x = \frac{m\pi}{L}$, $k_z = n\pi$, $k^2 = k_x^2 + k_z^2$, and $m, n = 1, 2, 3, \dots$. The corresponding eigenfunction takes the form

$$\begin{pmatrix} \psi \\ \theta \\ \phi \end{pmatrix} = \begin{pmatrix} A \\ B \\ C \end{pmatrix} e^{ik_x x} \sin k_z z e^{i\Omega_{\text{Hopf}} t} + \text{c.c.}, \quad (8)$$

where A, B, C are readily determined. One can show that R_t^{Hopf} is smallest in magnitude for $n = 1$. The integer mode number $m = M$, which minimizes R_t^{Hopf} , cannot be determined analytically, but will correspond to the integer lying closest to the real number $m = M^*$ satisfying $dR_t^{\text{Hopf}}/dm = 0$. Note that $M \sim M^* \sim O(L)$.

The linear modes (8) have the following symmetry properties:

$$\begin{aligned} \kappa_1 \begin{pmatrix} \psi \\ \theta \\ \phi \end{pmatrix} &= (-1)^m \begin{pmatrix} \psi \\ \theta \\ \phi \end{pmatrix}; \\ \kappa_2 \begin{pmatrix} \psi \\ \theta \\ \phi \end{pmatrix} &= (-1)^{m+n} \begin{pmatrix} \psi \\ \theta \\ \phi \end{pmatrix}, \end{aligned} \quad (9)$$

the crucial feature being that the first two modes of the system to become unstable ($m, m + 1$) will have opposite parity under reflections (either left-right or midplane). The justification for restricting attention in what follows to the interaction of these two modes is discussed in detail in [1].

C. The minimal system

The goal now is to derive a set of amplitude equations governing the behavior of these first two critical modes near onset of the oscillatory instability. In theory, this could be done by first writing the fields ψ, θ, ϕ as an arbitrary (infinite) sum of spatial modes, deriving a set of coupled modal equations, and then performing a center (or center-unstable) manifold reduction [14]. This proves inconvenient in practice, however. Instead, we make use of the fact that all modes will not contribute equally to the reduced center manifold equations. In particular, if the center manifold equations are to be truncated at order N , then only spatial modes that are of order $N - 1$ or less will contribute to the truncated equations. For our purposes, since we wish to determine the center manifold equations only through cubic order, the relevant spatial modes can be determined as follows: first express the fields ψ, θ, ϕ as a linear combination of the critical modes $m, m + 1$ (the vertical mode number will be $n = 1$ for both modes). The second order modes generated from the nonlinear interaction terms in equations (3a)–(3c), $J(\psi, \nabla^2 \psi), J(\psi, \theta), J(\psi, \phi)$, are then determined. Only these modes need be retained for the modal expansion; all other modes can then be neglected. We find (cf. [15])

$$\begin{aligned} \psi &= a_m(t) \sin\left(\frac{m\pi}{L}x\right) \sin(\pi z) + a_{m+1}(t) \sin\left(\frac{(m+1)\pi}{L}x\right) \sin(\pi z) \\ &\quad + a_1(t) \sin\left(\frac{\pi}{L}x\right) \sin(2\pi z) + a_{2m+1}(t) \sin\left(\frac{(2m+1)\pi}{L}x\right) \sin(2\pi z), \\ \theta &= b_m(t) \cos\left(\frac{m\pi}{L}x\right) \sin(\pi z) + b_{m+1}(t) \cos\left(\frac{(m+1)\pi}{L}x\right) \sin(\pi z) + b_0(t) \sin(2\pi z) + b_1(t) \cos\left(\frac{\pi}{L}x\right) \sin(2\pi z) \\ &\quad + b_{2m+1}(t) \cos\left(\frac{(2m+1)\pi}{L}x\right) \sin(2\pi z) \\ \phi &= c_m(t) \cos\left(\frac{m\pi}{L}x\right) \sin(\pi z) + c_{m+1}(t) \cos\left(\frac{(m+1)\pi}{L}x\right) \sin(\pi z) \\ &\quad + c_0(t) \sin(2\pi z) + c_1(t) \cos\left(\frac{\pi}{L}x\right) \sin(2\pi z) + c_{2m+1}(t) \cos\left(\frac{(2m+1)\pi}{L}x\right) \sin(2\pi z), \end{aligned} \quad (10)$$

where $a_m, b_m, c_m, a_{m+1}, b_{m+1}, c_{m+1}, a_1, b_1, c_1, b_0, c_0, a_{2m+1}, b_{2m+1}, c_{2m+1}$ are the amplitudes for the relevant spatial modes. Note that, in contrast to the corresponding equations for an unbounded system [16, 17], there are no terms representing mean flows and all the amplitudes are *real*. Substituting into the governing equations and neglecting all spatial harmonics not already included now yields a system of 14 coupled equations [15]:

$$\begin{aligned}
\frac{da_m}{dt} &= -\sigma a_m + \frac{LmR_t\sigma}{(L^2+m^2)\pi} b_m - \frac{LmR_s\sigma}{(L^2+m^2)\pi} c_m \\
&\quad + \frac{(1+2m)(-3L^2+2m+m^2)\pi^2}{4L(L^2+m^2)} a_{m+1}a_1 + \frac{(3L^2+2m+3m^2)\pi^2}{4L(L^2+m^2)} a_{m+1}a_{2m+1}, \\
\frac{db_m}{dt} &= \frac{m\pi}{L} a_m - \frac{(L^2+m^2)\pi^2}{L^2} b_m \\
&\quad + \frac{\pi^2}{4L} a_{2m+1}b_{m+1} + \frac{\pi^2}{4L} a_{m+1}b_{2m+1} + \frac{m\pi^2}{L} a_m b_0 + \frac{(1+2m)\pi^2}{4L} a_1 b_{m+1} + \frac{(1+2m)\pi^2}{4L} a_{m+1} b_1, \\
\frac{dc_m}{dt} &= \frac{m\pi}{L} a_m - \frac{(L^2+m^2)\pi^2\tau}{L^2} c_m \\
&\quad + \frac{\pi^2}{4L} a_{2m+1}c_{m+1} + \frac{\pi^2}{4L} a_{m+1}c_{2m+1} + \frac{m\pi^2}{L} a_m c_0 + \frac{(1+2m)\pi^2}{4L} a_1 c_{m+1} + \frac{(1+2m)\pi^2}{4L} a_{m+1} c_1, \\
\frac{da_{m+1}}{dt} &= -\sigma a_{m+1} + \frac{L(m+1)R_t\sigma}{(L^2+m^2+2m+1)\pi} b_{m+1} - \frac{L(m+1)R_s\sigma}{(L^2+m^2+2m+1)\pi} c_{m+1} \\
&\quad + \frac{(1+2m)(3L^2-m^2+1)\pi^2}{4L(L^2+m^2+2m+1)} a_m a_1 + \frac{(3L^2+3m^2+4m+1)\pi^2}{4L(L^2+m^2+2m+1)} a_m a_{2m+1}, \\
\frac{db_{m+1}}{dt} &= \frac{(m+1)\pi}{L} a_{m+1} - \frac{(L^2+m^2+2m+1)\pi^2}{L^2} b_{m+1} \\
&\quad - \frac{\pi^2}{4L} a_{2m+1}b_m - \frac{\pi^2}{4L} a_m b_{2m+1} + \frac{(m+1)\pi^2}{L} a_{m+1} b_0 - \frac{(1+2m)\pi^2}{4L} a_1 b_m + \frac{(1+2m)\pi^2}{4L} a_m b_1, \\
\frac{dc_{m+1}}{dt} &= \frac{(m+1)\pi}{L} a_{m+1} - \frac{(L^2+m^2+2m+1)\pi^2\tau}{L^2} c_{m+1} \\
&\quad - \frac{\pi^2}{4L} a_{2m+1}c_m - \frac{\pi^2}{4L} a_m c_{2m+1} + \frac{(m+1)\pi^2}{L} a_{m+1} c_0 - \frac{(1+2m)\pi^2}{4L} a_1 c_m + \frac{(1+2m)\pi^2}{4L} a_m c_1, \\
\frac{da_1}{dt} &= -\sigma a_1 - \frac{(1+2m)^2\pi^2}{4L(1+4L^2)} a_m a_{m+1} - \frac{LR_s\sigma}{(1+4L^2)\pi} c_1 + \frac{LR_t\sigma}{(1+4L^2)\pi} b_1, \\
\frac{db_1}{dt} &= \frac{\pi}{L} a_1 - \frac{(1+4L^2)\pi^2}{L^2} b_1 - \frac{(1+2m)\pi^2}{4L} a_{m+1}b_m - \frac{(1+2m)\pi^2}{4L} a_m b_{m+1}, \\
\frac{dc_1}{dt} &= \frac{\pi}{L} a_1 - \frac{(1+4L^2)\pi^2\tau}{L^2} c_1 - \frac{(1+2m)\pi^2}{4L} a_{m+1}c_m - \frac{(1+2m)\pi^2}{4L} a_m c_{m+1}, \\
\frac{da_{2m+1}}{dt} &= -\sigma a_{2m+1} + \frac{L(1+2m)R_t\sigma}{(4L^2+4m^2+4m+1)\pi} b_{2m+1} - \frac{L(1+2m)R_s\sigma}{(4L^2+4m^2+4m+1)\pi} c_{2m+1} \\
&\quad + \frac{(1+2m)\pi^2}{4L(4L^2+4m^2+4m+1)} a_m a_{m+1}, \\
\frac{db_{2m+1}}{dt} &= \frac{(1+2m)\pi}{L} a_{2m+1} - \frac{(4L^2+4m^2+4m+1)\pi^2}{L^2} b_{2m+1} - \frac{\pi^2}{4L} a_{m+1}b_m + \frac{\pi^2}{4L} a_m b_{m+1}, \\
\frac{dc_{2m+1}}{dt} &= \frac{(1+2m)\pi}{L} a_{2m+1} - \frac{(4L^2+4m^2+4m+1)\pi^2\tau}{L^2} c_{2m+1} - \frac{\pi^2}{4L} a_{m+1}c_m + \frac{\pi^2}{4L} a_m c_{m+1}, \\
\frac{db_0}{dt} &= -4\pi^2 b_0 - \frac{m\pi^2}{2L} a_m b_m - \frac{(m+1)\pi^2}{2L} a_{m+1} b_{m+1}, \\
\frac{dc_0}{dt} &= -4\pi^2\tau c_0 - \frac{m\pi^2}{2L} a_m c_m - \frac{(m+1)\pi^2}{2L} a_{m+1} c_{m+1}.
\end{aligned} \tag{11}$$

These equations constitute the *minimal* system for the present problem; cf. [17].

Note first that, since $m \sim O(L)$ and L is large, several of the terms in these equations will not contribute significantly. Second, observe that the equations are equivariant under the reflection symmetries κ_1, κ_2 , whose group actions now take the form

$$\begin{aligned}
\kappa_1 : & [a_m, b_m, c_m, a_{m+1}, b_{m+1}, c_{m+1}, a_1, b_1, c_1, a_{2m+1}, b_{2m+1}, c_{2m+1}, b_0, c_0] \\
& \rightarrow [(-1)^m a_m, (-1)^m b_m, (-1)^m c_m, (-1)^{m+1} a_{m+1}, (-1)^{m+1} b_{m+1}, \\
& \quad (-1)^{m+1} c_{m+1}, -a_1, -b_1, -c_1, -a_{2m+1}, -b_{2m+1}, -c_{2m+1}, b_0, c_0]
\end{aligned} \tag{12a}$$

$$\begin{aligned} \kappa_2 : & [a_m, b_m, c_m, a_{m+1}, b_{m+1}, c_{m+1}, a_1, b_1, c_1, a_{2m+1}, b_{2m+1}, c_{2m+1}, b_0, c_0] \\ & \rightarrow [(-1)^{m+1}a_m, (-1)^{m+1}b_m, (-1)^{m+1}c_m, (-1)^m a_{m+1}, (-1)^m b_{m+1}, \\ & (-1)^m c_{m+1}, -a_1, -b_1, -c_1, -a_{2m+1}, -b_{2m+1}, -c_{2m+1}, b_0, c_0]. \end{aligned} \quad (12b)$$

Lastly, if Eqs. (11) are linearized about the origin (i.e., about the trivial conducting solution), then the groups of modes indexed by $m, m+1, 1, 2m+1, 0$ decouple from one another. For example, the linearized equations for mode m are

$$\begin{pmatrix} \frac{da_m}{dt} \\ \frac{db_m}{dt} \\ \frac{dc_m}{dt} \end{pmatrix} = \begin{pmatrix} -\sigma & \frac{LmR_s\sigma}{(L^2+m^2)\pi} & -\frac{LmR_s\sigma}{(L^2+m^2)\pi} \\ \frac{m\pi}{L} - \frac{(L^2+m^2)\pi^2}{L^2} & & 0 \\ \frac{m\pi}{L} & 0 & -\frac{\tau(L^2+m^2)\pi^2}{L^2} \end{pmatrix} \begin{pmatrix} a_m \\ b_m \\ c_m \end{pmatrix}. \quad (13)$$

One may verify that the above Jacobian matrix has a pure imaginary pair of eigenvalues $\pm i\Omega_m$ precisely for $R_t = R_t^{\text{Hopf}}$ given in (7a). Similar expressions, obtained by replacing m by $m+1$, hold for mode $m+1$.

D. Center-unstable manifold reduction

We wish to perform, following [14], a center (-unstable) manifold reduction for R_t close to the critical Rayleigh number for the second mode to go unstable. To do so, we first put the system into Jordan canonical form. Let $\delta_m, \bar{\delta}_m, \lambda_m$ denote the eigenvalues of the linear matrix in (13), and $\delta_{m+1}, \bar{\delta}_{m+1}, \lambda_{m+1}$ be the corresponding eigenvalues associated with mode $m+1$. For both modes, since R_t is close to its critical value for an oscillatory instability, we have $\delta_m, \delta_{m+1} \approx i\Omega$. These relations are only approximate, however, since the two modes do not bifurcate simultaneously. Thus when the second mode loses stability the nearly pure imaginary eigenvalue of the first will in general have a small positive real part. This setup forms the basis of the center-unstable manifold reduction to follow. The remaining eigenvalues, λ_m, λ_{m+1} , are strictly negative, and are given by

$$\lambda_m = -[\sigma + \pi^2(1 + \tau)(m^2 + L^2)/L^2], \quad (14)$$

with λ_{m+1} obtained by replacing m by $m+1$.

We next define new coordinates (z_m, \bar{z}_m, q_m) by

$$\begin{pmatrix} a_m \\ b_m \\ c_m \end{pmatrix} = \begin{pmatrix} A_{\delta_m} & A_{\bar{\delta}_m} & A_{\lambda_m} \\ B_{\delta_m} & B_{\bar{\delta}_m} & B_{\lambda_m} \\ C_{\delta_m} & C_{\bar{\delta}_m} & C_{\lambda_m} \end{pmatrix} \begin{pmatrix} z_m \\ \bar{z}_m \\ q_m \end{pmatrix}, \quad (15)$$

where the transformation elements $(A_{\delta_m}, \dots, C_{\lambda_m})$ are defined as follows:

$$A_{\sigma_m} = \sigma_m + \pi^2(L^2 + m^2)/L^2, \quad (16a)$$

$$B_{\sigma_m} = \pi m/L \quad (16b)$$

$$C_{\sigma_m} = \frac{\pi R_t m}{R_s L} - \frac{\pi(\sigma + \sigma_m)(L^2 + m^2)[\pi^2(L^2 + m^2) + L^2\sigma_m]}{R_s \sigma L^3 m}. \quad (16c)$$

Similar expressions, obtained by replacing m by $m+1$, define $(z_{m+1}, \bar{z}_{m+1}, q_{m+1})$. The inverse transformation corresponding to (15) will be denoted by

$$\begin{pmatrix} A_{\delta_m}^{-1} & A_{\bar{\delta}_m}^{-1} & A_{\lambda_m}^{-1} \\ B_{\delta_m}^{-1} & B_{\bar{\delta}_m}^{-1} & B_{\lambda_m}^{-1} \\ C_{\delta_m}^{-1} & C_{\bar{\delta}_m}^{-1} & C_{\lambda_m}^{-1} \end{pmatrix}. \quad (17)$$

The transformation (17) diagonalizes to lowest order the equations for the critical linear modes, yielding

$$\frac{dz_m}{dt} = \delta_m z_m + (\text{higher-order terms}), \quad (18a)$$

$$\frac{dz_{m+1}}{dt} = \delta_{m+1} z_{m+1} + (\text{higher-order terms}), \quad (18b)$$

along with the equations for the slaved modes

$$\frac{dq_m}{dt} = \lambda_m q_m + (\text{higher-order terms}), \quad (19a)$$

$$\frac{dq_{m+1}}{dt} = \lambda_{m+1} q_{m+1} + (\text{higher-order terms}) \quad (19b)$$

(in addition to the 8 other slaved modes $\frac{da_1}{dt}, \dots, \frac{dc_0}{dt}$). Using symmetry considerations [see (12a)–(12b)] the center-unstable manifold can now be written (through quadratic order) as

$$\begin{aligned} q_m &= 0, \\ q_{m+1} &= 0, \\ a_1 &= \alpha_1 z_m z_{m+1} + \alpha_2 z_m \bar{z}_{m+1} + \text{c.c.}, \\ b_1 &= \beta_1 z_m z_{m+1} + \beta_2 z_m \bar{z}_{m+1} + \text{c.c.}, \\ c_1 &= \gamma_1 z_m z_{m+1} + \gamma_2 z_m \bar{z}_{m+1} + \text{c.c.}, \\ a_{2m+1} &= \alpha_3 z_m z_{m+1} + \alpha_4 z_m \bar{z}_{m+1} + \text{c.c.}, \\ b_{2m+1} &= \beta_3 z_m z_{m+1} + \beta_4 z_m \bar{z}_{m+1} + \text{c.c.}, \\ c_{2m+1} &= \gamma_3 z_m z_{m+1} + \gamma_4 z_m \bar{z}_{m+1} + \text{c.c.}, \\ b_0 &= \beta_5 |z_m|^2 + \beta_6 |z_{m+1}|^2 + \{\beta_7 z_m^2 + \beta_8 z_{m+1}^2 + \text{c.c.}\}, \\ c_0 &= \gamma_5 |z_m|^2 + \gamma_6 |z_{m+1}|^2 + \{\gamma_7 z_m^2 + \gamma_8 z_{m+1}^2 + \text{c.c.}\}. \end{aligned} \quad (20)$$

Substituting these equations into the equations of motion allows one to find explicitly the center-unstable equations for the critical modes (z_m, z_{m+1}) . The resulting equations are necessarily equivariant under both reflection symmetries of the original system. These symmetries now take the form $z_m \rightarrow -z_m$ and $z_{m+1} \rightarrow -z_{m+1}$. (Note that these are both exact symmetries of the system, but even if the midplane reflection symmetry is absent, it will “reappear” as a normal form symmetry.) The center-unstable equations can now be put into normal form. These calculations are quite lengthy and we do not reproduce them here. The final result is equations of the form (1a) and (1b) where

$$K_1 \approx K'_1 \approx H_1 + 2H_2, \quad (21a)$$

$$K_2 \approx K'_2 \approx H_1 + 3H_2, \quad (21b)$$

$$K_3 \approx K'_3 \approx H_1 + H_2. \quad (21c)$$

The quantities H_1, H_2 are given by

$$H_1 \equiv -\frac{\pi^4 m^2 |A_{\delta_m}|^2 B_{\delta_m} A_{\delta_m}^{-1}}{4 L^2 i\Omega + 2\pi^2} - \frac{\pi^4 m^2 |A_{\delta_m}|^2 C_{\delta_m} A_{\lambda_m}^{-1}}{4 L^2 i\Omega + 2\pi^2 \tau}, \quad (22a)$$

$$H_2 \equiv -\frac{\pi^2 m^2 (A_{\delta_m} B_{\delta_m} + A_{\delta_m} B_{\delta_m}) A_{\delta_m} A_{\delta_m}^{-1}}{16 L^2} - \frac{\pi^2 m^2 (A_{\delta_m} C_{\delta_m} + A_{\delta_m} C_{\delta_m}) A_{\delta_m} A_{\lambda_m}^{-1}}{16\tau L^2}. \quad (22b)$$

In Eqs. (21a)–(21c) and (22a) and (22b) only the leading order terms have been included; by explicit computation these are all of $O(1)$ in the limit $L \rightarrow \infty$. The $O(1/L)$ corrections to these coefficients have been calculated, but are not presented here (though they are included in the numerical simulations that follow).

We mention one remarkable feature of the normal form coefficients. The quantity H_2 turns out to be purely imaginary, and hence the real parts of all the nonlinear coefficients are equal [to within $O(1/L)$!]. As a result the coefficients violate the nondegeneracy condition $\text{Re}K_1 \neq \text{Re}K_2$ required of the D_4 -symmetric problem (assuming $|H_1|^2 + 2H_1 H_2 < 0$). When this condition fails the even parity standing wave in the D_4 -symmetric problem has a pair of purely imaginary eigenvalues and consequently the system is highly sensitive to perturbations, be they higher order terms or ones that break the D_4 symmetry. We speculate that this degeneracy might be related to the fact that for doubly diffusive convection in an unbounded system, the amplitude of the pure traveling wave solutions grows as $(R_t - R_t^{\text{Hopf}})^{\frac{1}{4}}$ instead of the usual $(R_t - R_t^{\text{Hopf}})^{\frac{1}{2}}$, owing to a degeneracy in a cubic normal form coefficient [6,13,17]. A second possibility is that it is associated with the particularly simple nature of the linear spatial eigenfunctions for this problem (due to the form of the boundary conditions).

III. NUMERICAL RESULTS

We briefly mention some results from numerical investigation of these normal form equations. Our choice of system parameter values is based on the experiments of Predtechensky *et al.* [6, 18]. We therefore looked at two

cases: *Case 1:* $\tau = 0.31, \sigma = 1.3 \times 10^5, R_s = 139, L = 20$; *case 2:* $\tau = 0.63, \sigma = 1.3 \times 10^5, R_s = 139, L = 20$. For each case we varied R_t over a range of values. In the simulations reported below all $O(1/L)$ corrections to the normal form coefficients (21a)–(21c) were retained. Only bifurcations leading to stable solutions are discussed.

Several comments are in order. First note that, since the Prandtl number is quite large, the mode number m that first goes unstable through an oscillatory bifurcation is $m \approx L$. The corresponding critical value of the Rayleigh number is $R_t \approx R_s + 4\pi^2(1 + \tau)$. Since the critical Rayleigh number for a steady state bifurcation is $4\pi^2 + R_s/\tau$, the oscillatory instability will set in first provided

$$R_s > \frac{4\pi^2 \tau^2}{1 - \tau}.$$

In case 1 the first mode to bifurcate from the origin has a critical Rayleigh number of 190.705 and wave number $m = 20$; the second mode ($m = 21$) bifurcates at $R_t = 190.827$. At $R_t = 190.84$, a stable standing wave solution $(z_{20}, 0)$ is present; an unstable standing wave $(0, z_{21})$ exists as well. At $R_t \approx 193.2$, two pairs of (stable/unstable) nonsymmetric stationary solutions of the form $(z_{20}, z_{21}), z_{20}z_{21} \neq 0$, appear through a saddle-node bifurcation. As discussed in [1], solutions of this type have a variety of appearances, depending on the precise values of the real and imaginary parts of z_{20}, z_{21} , but they all exhibit some propagative dynamics. Although in the following we refer to these collectively as traveling waves it is possible to distinguish two types of such waves, those that approach a pure traveling wave at large amplitude ($z_m \rightarrow \pm z_{m+1}$) and those that approach a mixed parity standing wave ($z_m \rightarrow \pm iz_{m+1}$). The stable traveling waves created at the saddle-node bifurcation are of the latter type. Our theory also contains traveling waves of the former type but these are unstable, in contrast to the Ginzburg-Landau prediction of stable (pure) traveling waves at large amplitude [6]. As R_t is increased beyond $R_t \approx 193.2$, the unstable traveling waves created in the saddle-node bifurcation migrate towards the still-stable standing wave, eventually colliding with it in a subcritical pitchfork bifurcation at $R_t \approx 193.3$. Thereafter only the stable traveling waves remain. Thus in the narrow interval [193.2, 193.3] both standing and traveling waves are stable, while for larger values of R_t only the traveling waves are stable. In Figs. 1 and 2 we show the oscillations of the stream function $\psi(x, z, t)$ for each of these states based on the representation (10)

$$\psi(x, z, t) = 2\text{Re} \left\{ A_{\delta_m} z_m(t) \sin \left[\frac{m\pi x}{L} \right] + A_{\delta_{m+1}} z_{m+1} \sin \left[\frac{(m+1)\pi x}{L} \right] \right\} \sin \pi z + (\text{higher-order terms}). \quad (23)$$

In interpreting the figures one must bear in mind that ψ is a pseudoscalar under reflection. Consequently an odd parity ψ describes an even mode and vice versa, as seen, for example, from the physical fields θ, ϕ . Thus Fig. 1(a),

obtained for case 1, shows an example of an even parity standing wave ($m = 20$), while Fig. 1(b) shows an odd parity standing wave ($m = 21$). These modes are the two primary modes of the system. Figure 2 shows the

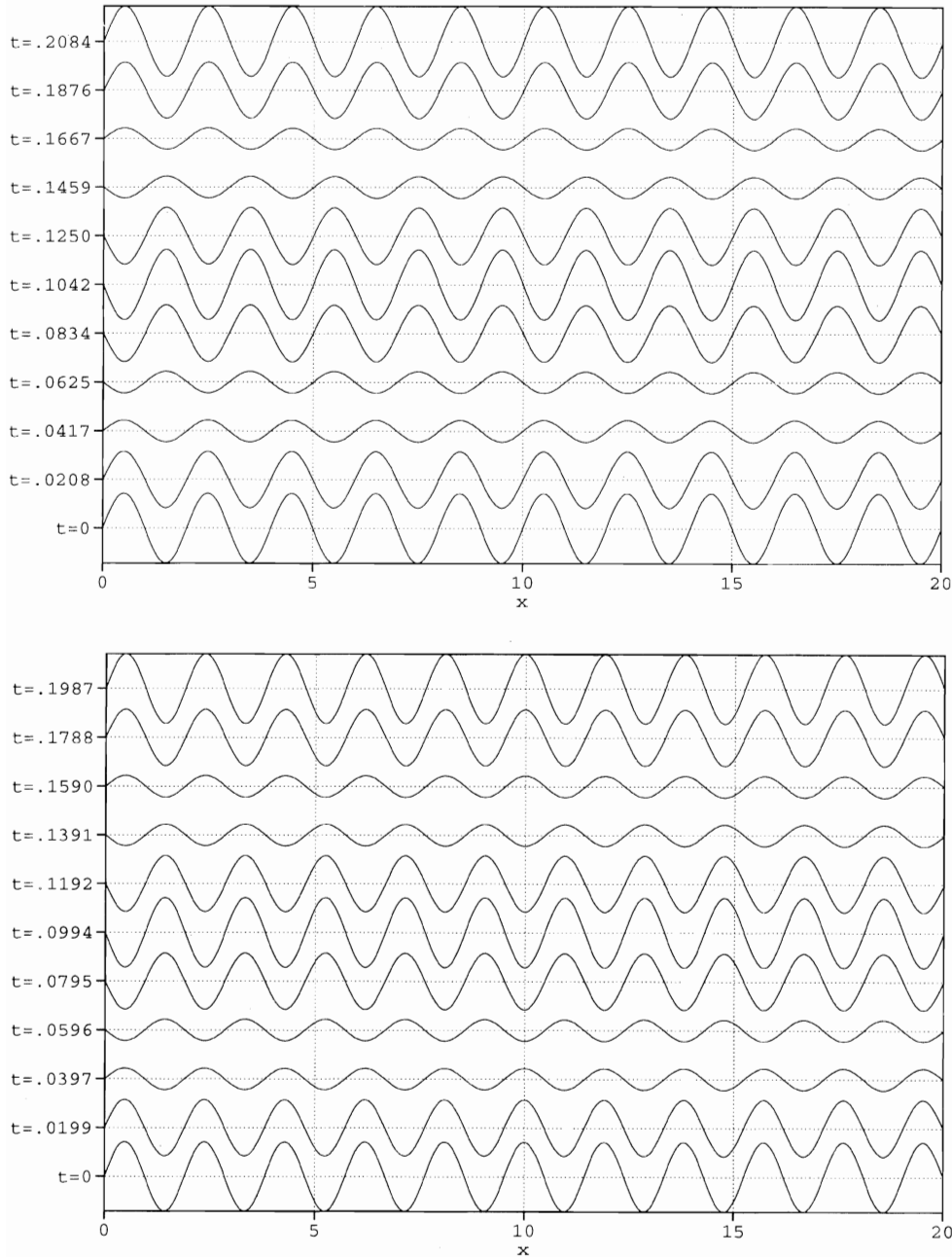


FIG. 1. Stable pure parity standing waves for case 1, with $R_t = 193.264$, in the stream function representation. Each wave is depicted for one oscillation period. (a) The $m = 20$ mode with amplitude 2.155; (b) the $m = 21$ mode with amplitude 2.139. The velocity field $(u, w) \equiv (-\psi_z, \psi_x)$ corresponding to (a) is even under reflection, but odd in (b).

mixed parity stream function characteristic of the traveling wave created at $R_t \approx 193.2$.

In case 2, the first mode ($m = 20$) goes unstable at $R_t \approx 203.348$, the second ($m = 21$) at 203.501. At $R_t = 203.363$, a stable standing wave solution is found. This solution persists for a range of Rayleigh numbers, but becomes unstable at $R_t \approx 205.70$ in a supercritical pitchfork bifurcation that produces a pair of stable traveling wave solutions. These solutions also approach a mixed parity standing wave at large amplitude (cf. Fig. 2). In neither of the cases examined have we found stable two-frequency “blinking” states of the type observed in the experiments. We also did not find any

of the more exotic behavior, including period doublings, repeated transients, and chaotic behavior seen in experiments on binary fluid convection [7, 8] and in numerical simulation of related partial differential equation [9, 10], even though Eqs. (1a) and (1b) do allow for such phenomena [1].

IV. DISCUSSION

In this paper we have presented a detailed derivation of the amplitude equations describing the onset of an oscillatory instability in a large aspect ratio continuum system. In contrast to earlier attempts to derive such equa-

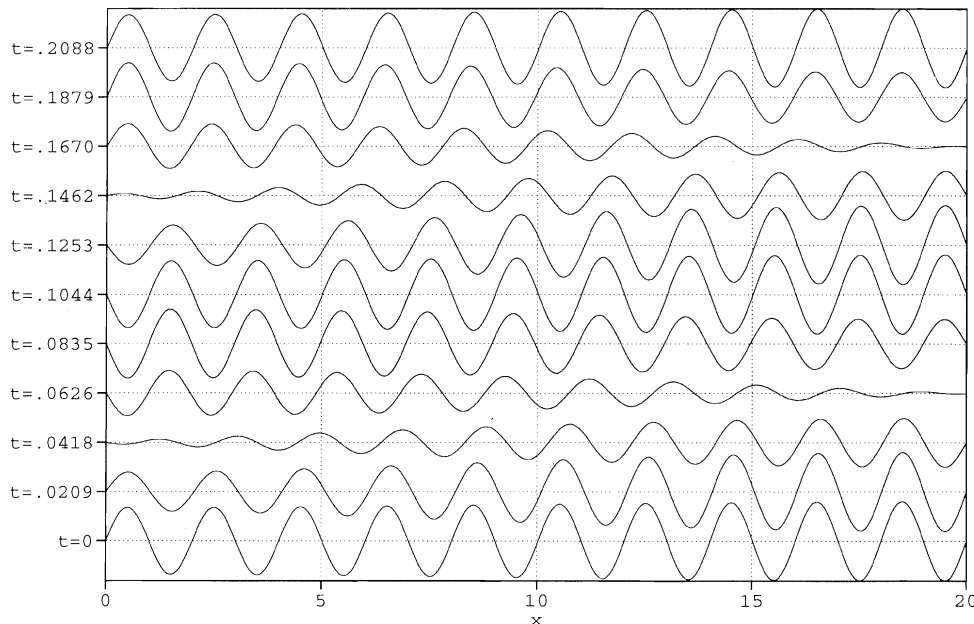


FIG. 2. Stable traveling wave for case 1 with $R_t = 193.264$, shown for one oscillation period.

tions as perturbations of the coupled Ginzburg-Landau equations describing the nonlinear interaction of left- and right-traveling waves in an unbounded system, we have considered the corresponding instability in a finite domain, and then specialized to the large aspect ratio limit. The resulting Eqs. (2a) and (2b), appropriate to this limit, contain additional nonlinear terms with $O(1)$ coefficients and hence do not constitute a small perturbation of the Ginzburg-Landau equations. The calculations of this paper thus provide an explicit verification of the conclusions of Ref. [1]. Although both approaches are able to describe qualitatively the type of dynamics that have been observed in experiments and in numerical simulations, we believe that only the approach adopted in this paper can ultimately be used to produce *quantitative* predictions for the experiments.

In this respect the direct comparison between the theoretical predictions made here on the basis of the normal form equations (1a) and (1b) and the actual experimental observations is disappointing. For example, in the experiments the observed traveling waves always eventually evolve into a large-amplitude “blinking state.” We do not find such stable, two-frequency (modulated) waves in the relevant parameter ranges in our numerical integration of the normal form equations (although we have observed modulated wavelike behavior in the form of long-lasting transients). Such differences are not unexpected at this stage, however, since our simplified starting model (3a)–(3c) does not incorporate several physical features that are present (to varying degrees) in the actual experiments. First, the model assumes an ideal Hele-Shaw geometry. However, in the experiments the actual ratio of the thickness (w) of the layer to its height (d) was not zero, but instead ranged from 0.254 to 0.069. The effect of finite w/d could be investigated by introducing a modified viscosity term in Eqs. (3a)–(3c), but we have not

done so. In addition to changing the computed values of the normal form coefficients such a term would also affect the appearance of the spatial wave forms. Second, cross-diffusion terms have not been included in the model. It is suspected [18] that in the experiments of Predtechensky *et al.* [6] the off-diagonal elements in the diffusion matrix can be as large as 10% of the diagonal one, and hence should not be neglected. Third, the degree to which the aspect ratio of the experimental system ($L = 20$) can be considered large (in an asymptotic sense) is unclear. Finally, as already mentioned, the potential degeneracy in the coefficients (22a) and (22b) suggests that in this problem the bifurcation behavior may not be completely determined by the third-order truncation of the normal form equations. We surmise that with the inclusion of the above effects, the normal form equations (1a) and (1b) could describe “blinking states” for the exact experimental parameters; such states are known to be present in Eqs. (1a) and (1b) in the absence of degeneracies [1]. In fact, based on our analytical results in the weakly nonlinear regime, we are in a position to postulate that the aforementioned effects, which are typically considered to be of only secondary importance, do indeed play an important role in the experiments of Predtechensky *et al.* [6].

In this connection we mention that the modal truncation (11) could provide a good model of the dynamics arising from the interaction between the even and odd modes even for parameters substantially far from those considered here. In particular this should be so for *finite* (or even moderate) aspect ratios, such as those employed in the experiments, for which the first two modes set in at substantially different Rayleigh numbers and consequently their interaction occurs at larger amplitudes. Moreover, the usefulness of Eqs. (11) should extend well into the Rayleigh number regime in which additional

modes are unstable, provided only that there are no secondary instabilities involving these modes. That this can be the case is demonstrated in Ref. [19] for a steady state instability in a finite domain. Although not exact, models of this type have proved in the past to be a valuable guide to both the experiments and to the interpretation of simulations of the full partial differential equations [20]. In particular the simulations by Jacqmin and Heminger [10] of closely related partial differential equations suggest that much of the behavior of interest involves a small number of spatial modes even relatively far above on-

set. These considerations indicate that Eqs. (11) merit further study.

ACKNOWLEDGMENTS

This work was supported in part by INCOR funds from Los Alamos National Laboratory and the National Science Foundation under Grant No. DMS-9406144. After the submission of this paper we learned of related work by Zangeneh [21] on oscillatory magnetoconvection in finite containers. We thank W. Nagata for this information.

-
- [1] A.S. Landsberg and E. Knobloch, preceding paper, Phys. Rev. E **53**, 3579 (1996).
 - [2] M. Bestehorn, R. Friedrich, and H. Haken, Z. Phys. B **77**, 151 (1989).
 - [3] W. Nagata, Proc. R. Soc. Edinburgh A **117**, 1 (1991).
 - [4] G. Dangelmayr and E. Knobloch, in *The Physics of Structure Formation: Theory and Simulation*, edited by W. Güttinger and G. Dangelmayr (Springer-Verlag, Berlin, 1987), pp. 387–393; G. Dangelmayr and E. Knobloch, Nonlinearity **4**, 399 (1991).
 - [5] G. Dangelmayr, E. Knobloch, and M. Wegelin, Europhys. Lett. **16**, 723 (1991).
 - [6] A.A. Predtechensky, W.D. McCormick, J.B. Swift, Z. Noszticius, and H.L. Swinney, Phys. Rev. Lett. **72**, 218 (1994); A.A. Predtechensky, W.D. McCormick, J.B. Swift, A. Rossberg, and H.L. Swinney, Phys. Fluids **6**, 3923 (1994).
 - [7] P. Kolodner, C.M. Surko, and H. Williams, Physica D **37**, 319 (1989); V. Steinberg, J. Fineberg, E. Moses, and I. Rehberg, *ibid.* **37**, 359 (1989).
 - [8] P. Kolodner, Phys. Rev. E **47**, 1038 (1993).
 - [9] A.E. Deane, E. Knobloch, and J. Toomre, Phys. Rev. A **37**, 1817 (1988).
 - [10] D. Jacqmin and J. Heminger (unpublished).
 - [11] M.G.M. Gomes and I. Stewart, in *Dynamics, Bifurcation and Symmetry: New Trends and New Tools*, edited by P. Chossat (Kluwer, Norwell, MA, 1994).
 - [12] D.A. Nield, Water Resources Res. **4**, 553 (1968).
 - [13] E. Knobloch, Phys. Rev. A **34**, 1538 (1986).
 - [14] D. Armbruster, J. Guckenheimer, and P. Holmes, SIAM J. Appl. Math. **49**, 676 (1987).
 - [15] E. Knobloch and J. Guckenheimer, Phys. Rev. A **27**, 408 (1983).
 - [16] E. Knobloch, A.E. Deane, and J. Toomre, Contemp. Math. **99**, 339 (1989).
 - [17] E. Knobloch and D.R. Moore, Phys. Rev. A **42**, 4693 (1990).
 - [18] A.A. Predtechensky (private communication).
 - [19] L.S. Tuckerman and D. Barkley, Physica D **46**, 57 (1990).
 - [20] E. Knobloch, M.R.E. Proctor, and N.O. Weiss, in *Turbulence in Fluid Flows: A Dynamical Systems Approach*, Vol. 55 of IMA Volumes in Mathematics and Its Applications, edited by G.R. Sell, C. Foias, and R. Temam (Springer-Verlag, New York, 1993), pp. 59–72.
 - [21] H.R.Z. Zangeneh, Ph.D thesis, University of British Columbia (1993).